

PREPARATION AND CHARACTERIZATION OF HIGH-DISPERSED Pt/C NANO-ELECTROCATALYSTS FOR FUEL CELL APPLICATIONS

Hoang Anh Huy¹, Tran Van Man², Huynh Thien Tai³, Van Thi Thanh Ho^{3,*}

¹*HoChiMinh City University of Technology, 268 Ly Thuong Kiet Street,
District 10, Ho Chi Minh City*

²*HoChiMinh City University of Science, 227 Nguyen Van Cu, District 5, Ho Chi Minh City*

³*HoChiMinh City University of Natural Resources and Environment, 236B Le Van Sy,
Tan Binh District, Ho Chi Minh City*

*Email: httvan@hcmunre.edu.vn

Received: 1 November 2015; Accepted for publication: 2 June 2016

ABSTRACT

Synthesis conditions are keys to control size and dispersion of Platinum (Pt) nanoparticle (NP) structures that are the most important factors in improving the electrochemical activity and durability of electrodes in low temperature fuel cells. In this study, five catalyst samples Pt nanoparticles on carbon support (Pt NPs/C) have been synthesized by the simple and facile method at 30 °C or 60 °C in pH = 6.5 or pH = 11 solution with or without using ethylene glycol (EG). The morphology, size, dispersion and activity of Pt NPs/C were characterized by using X-ray diffraction (XRD), Transmission electron microscopy (TEM) and Cyclic Voltammetry (CV) in order to evaluate the effectiveness of this synthesis process. We found that the size, morphology and dispersion of Pt NPs/C were strongly affected by adjusting the temperature, pH and the presence of ethylene glycol. Finally, through determining electrochemically active surface area of a typical catalytic sample, we were able to conclude that the procedure have been established to reach goals simple, inexpensive but still can improve the catalytic activity for methanol oxidation reaction in direct methanol fuel cell (DMFC).

Keywords: Pt/C, Pt nanoparticles, Pt electrochemical active surface area, Pt/C catalyst, PtNPs/C.

1. INTRODUCTION

Platinum is one of the most active metal catalysts at room temperature for electrochemical reactions of fuel cells. Its activity is strongly dependent on the shape, size and particles' size distribution which can be controlled through synthesis conditions as the temperature, pH and enhancer. In practical cases, highly dispersed Pt catalysts with large surface areas are extremely important to increase the electrocatalytic activity [1, 2]. To achieve a catalytic surface area large and high activity, it requires understanding the relationship between the catalytic activity and their structure/composition, which are the basis for rational design of highly efficient

electrocatalysts for fuel cells and other electrochemical processes. The conventional preparation techniques based on wet impregnation and the chemical reduction of metal precursors do not provide satisfactory control of particle shape and size as well as the distribution of Pt particles on carbon support [3]. Synthesis of highly dispersed supporting platinum with uniform nanoparticle size still remains a challenge, especially for high metal loading. The conventional methods for the synthesis of Ptelectrocatalyst are mainly impregnation and colloid methods such as sulfite complex route and the colloidal route, the impregnation method usually produces NPs with large average particle sizes and broad size distributions while the colloidal route produces well-homogenized ultrafine Ptelectrocatalysts, however, the complexity of the latter hinders its utilization [4]. Many investigators have contributed many efforts to search alternative routes.

So far, there have been attempting to develop alternative synthesis methods based on microemulsions [5], sonochemistry [6] and microwave irradiation [7, 8], all of which are in principle more conducive to produce colloids and clusters on the nanoscale, and with greater uniformity.

In this study, a simple procedure for preparing Pt metal nanoparticles supported on carbon is reported. The uniform platinum nanoparticles supported on carbon with Pt loading up to 40 wt% that is a standard amount in order to obtain higher dispersion and smaller crystallites [9]. This study set the stage for further inspections with the desire to create the best possible Pt/C catalyst. Through this work, we found that the optimize preparation is simple, fast but it is able to control the particle size and distribution of Pt particles on the carbon support and could enhance the activity of catalyst for fuel cell applications.

2. EXPERIMENTAL SECTION

2.1. Material used

Vulcan XC-72R carbon with particle size ~ 60 nm using as a support was purchased from Fuel Cell Store (USA). All the chemicals were of analytical grade; D521 Nafion Dispersion - Alcohol based 1100 EW at 5 wt%, Ethyl alcohol pure (≥ 99.5 %, Acros), Hydrogen hexachloroplatinate (IV) hexahydrate, 99.9 %, (trace metal basis), 38 to 40 % Pt($\text{H}_2\text{PtCl}_6 \cdot 6\text{H}_2\text{O}$), ethylene glycol (EG), acetone branded Acros (Belgium), sodium borohydride (NaBH_4), nitric acid (HNO_3) (65 % - 68 %) (China), Sulfuric acid (95.0 - 98.0 %) were used.

2.2. Preparation of pre-treated Vulcan XC-72R

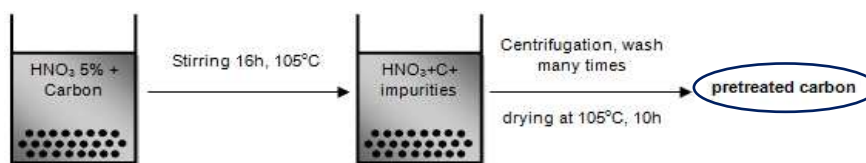


Figure 1. Preparation procedure of pre-treated Vulcan XC-72R.

Vulcan XC-72R carbon powder was treated to clean the contaminant in the commercial carbon. For example, 0.5 g carbon was dispersed in a round bottom flask with 500 mL of the 5 % HNO_3 solution, the mixture was refluxed for 16 hours at 105 °C. Treated carbons were centrifuged with 4500 rpm for several times with each 5 minutes for washing with de-ionized

(DI) water and acetone (15 mL H₂O or Acetone for each centrifuge tubes), then dried at 105 °C in an oven for 10 hours (Fig. 1) [10].

2.3. Preparation of Pt/C catalysts

Pt/C catalysts particles were synthesized by the following route: Pt particles were dispersed on the carbon supports by the following process: 50 mg treated carbon was dispersed into the solvent (DI water with and without using EG), 3.39 mL H₂PtCl₆·6H₂O with concentration 0.05 M into the mixed precursor. The pH of this mixture was adjusted to 6.5 and 11 by drop wise addition of NaOH 0.1N solution. The mixture was stirred for 5 min and ultrasonicated for 15 minutes at room temperature. Then an excess amount of reduction agent 6.84 mL NaBH₄ 0.05 M was added and the mixture was stirred by using a magnetic bar under atmospheric pressure at room temperature or 60 °C for 2 hours (Fig. 2).

Finally, the synthesized catalyst particles Pt/C were washed by DI water, centrifuged and dried for 12 hours at 100 °C [11]. All samples are shown in the Table 1.

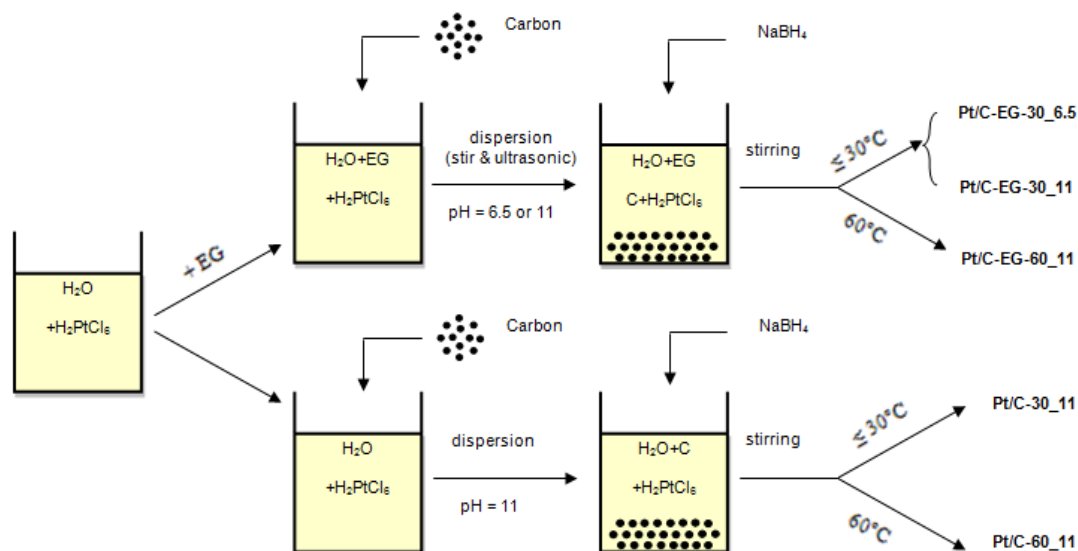


Figure 2. The preparation of 40 wt% Pt/C with different conditions (pH, temperature, using with and without EG).

2.4. XRD, TEM and CV Analysis

The samples were characterized by using X-ray diffraction (XRD), Transmission electron microscopy (TEM), Cyclic voltammetry (CV) in order to assess catalytic activity of Pt particles through the effects of ethylene glycol, pH and temperature on the morphology, size and dispersion of platinum nanoparticles catalyst on carbon support for fuel cells.

X-ray powder diffraction (XRD) patterns were recorded by using a Cu K α radiation source on a D8 Advance Bruker powder diffractometer (University of Technology-VNU HCM City). Transmission electron microscope (TEM) was taken by JEM-1400 (JEOL, Japan), (University of Technology-VNU HCM City). Cyclic Voltammetry (CV) was recorded by AutoLab machine system at Applied Physical Chemistry Laboratory, University of Science, VNU-HCM, Vietnam.

3. RESULTS AND DISCUSSION

The samples of 40 wt% Pt/C catalysts were prepared with various conditions (Table 1). The effect of parameters such as EG, temperature as well as pH on the size, distribution of Pt NPs on carbon were studied. The samples were synthesized with and without using EG, carried out at room temperature (30 °C) and 60 °C. The influence of pH value was also studied at 6.5 and 11.

Table 1. The samples of 40 wt% Pt/C catalysts were prepared with various conditions.

Ethylene glycol (EG)	Temperature (°C)	pH	Catalysts
-	30	11	Pt/C-30_11
EG	30	11	Pt/C-EG-30_11
EG	30	6.5	Pt/C-EG-30_6.5
EG	60	11	Pt/C-EG-60_11
-	60	11	Pt/C-60_11

3.1. X-ray powder diffraction (XRD)

The 40 wt% Pt/C samples are synthesized with the presence of EG and without EG at the room temperature and 60 °C in pH = 6.5 and 11 solutions. X-ray diffraction of these samples were shown in the Fig. 3. They indicated that all the broad diffraction peaks of the XRD patterns at $2\theta = 39.6, 47.4, 67.1^\circ$, corresponding to the reflections (111), (200), (220), respectively, which are consistent with the face centered cubic (fcc) structure of platinum (Pt), can be assigned to (JCPDS Card 04-0802), thus demonstrating the presence of crystalline Pt [12]. In addition, a broad peak at $2\theta \approx 25^\circ$ was observed but not clearly due to the (002) plane of the hexagonal structure of the carbon support (Vulcan XC-72R) is amorphous carbon with small regions of graphitic properties [13].

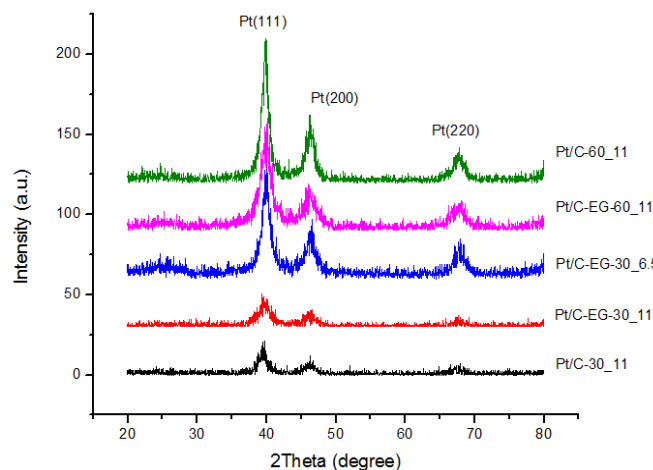


Figure 3. X-ray diffraction (XRD) patterns of 40 wt% Pt/C catalysts.

Table 2, the Pt/C sample with the presence of EG showed wider peak than the remaining samples in the preparation process, suggesting the Pt particles size of sample using EG, pH = 11 at room temperature (30 °C) is smallest (3.84 nm), (estimated from the Scherrer formula at Pt

(111) peak). The largest active surface area of Pt is observed for sample Pt/C-EG-30_11 compared to other samples due to the small particle size of Pt as well as the highly dispersed Pt on the carbon support ($73 \text{ m}^2/\text{g}_{\text{Pt}}$) [14].

Scherrer equation:

$$B(2\theta) = \frac{K\lambda}{L \cos\theta} \longrightarrow L = \frac{0.9\lambda}{B \cos\theta} \quad (*)$$

where, L = average crystal size (angstrom or nm); B = the full width half maximum of the peak; K = the Scherrer constant; depends on how the width is determined, the shape of the crystal, and the size distribution; λ = the wavelength of the radiation used to collect the data.

We used the Pt (111) plane to determine the average crystallite size. The FWHM is calculated from the (111) peak by using Originlab software. The value of K is 0.9 due to the structure of Pt's face-centered cubic and the wavelength used to be $\lambda_{\text{Cu}} = 1.54 \text{ \AA}$.

Surface areas of crystalline Pt were also calculated from the crystallite size using the following equation:

$$S = \frac{6000}{\rho d} \quad (**)$$

where, d is the average crystallite size (nm), S is the average surface area ($\text{m}^2 \text{ g}^{-1}$) and ρ is the density of Pt (21.4 g cm^{-3}). The sizes and surface areas are summarized in Table 2.

Table 2. The average crystallite size and surface area were estimated from (*) and (**).

Catalysts	L_{XRD} (nm)	S_{XRD} ($\text{m}^2/\text{g}_{\text{Pt}}$)
Pt/C-30_11	7.14	39.3
Pt/C-EG-30_11	3.84	73
Pt/C-EG-30_6.5	7.72	36.3
Pt/C-EG-60_11	5.85	48
Pt/C-60_11	9.16	30.6

3.2. Transmission electron microscope (TEM)

TEM picture and histogram of particle size distribution (Fig. 4) were consistent with calculating the crystallite size of Pt nanoparticles catalyst from the samples' XRD result. The TEM size d_{TEM} was determined using the following equation:

$$d_{\text{TEM}} = \frac{\sum_{i=1}^n n_i d_i}{n} \quad (***)$$

where, n is the total number of measured particles, n_i is the number of particles with a size d_i .

The size and surface area (S_{TEM}) were estimated from TEM are shown in Table 3.

The Pt/C-EG-30_11 catalyst prepared using NaBH_4 as the reducing agent in EG solution at $\text{pH} = 11$ has demonstrated that its particles size is smallest, the largest size belongs to Pt/C-60_11 catalyst and particles size decreased in the following sequence: Pt/C-60_11 > Pt/C-EG-30_6.5 > Pt/C-30_11 > Pt/C-EG-60_11 > Pt/C-EG-30_11, (Table 3). The presence of ethylene glycol (EG) supported Pt nanoparticles not only have narrow size, but they also distribute uniformly on carbon support (Fig. 4. (c), (e), (g)). This has been reported that the reaction with

the attendance of EG and NaBH₄ in a solution will form a complex reducing solution, and EG has performed roles as both a reducing agent for Pt reduction and a stabilizing for the reduced Pt nanoparticles [15].

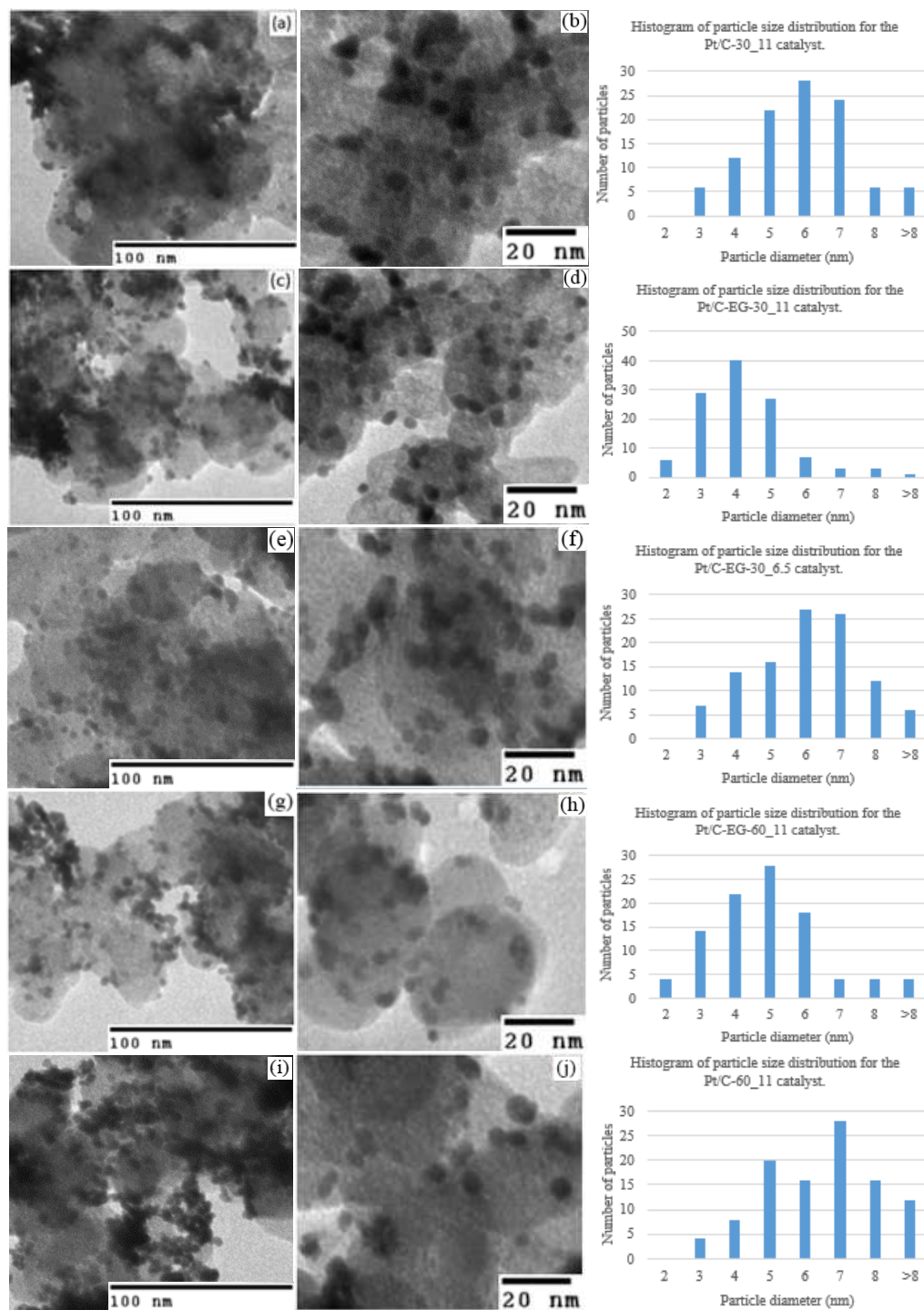


Figure 4. TEM pictures and histograms of particle size distribution for patterns of 40 wt% Pt/C catalysts.

However, when the temperature increases from room temperature to 60 °C, there is a significant difference in the crystallinity and the particles size of Pt on carbon. The Pt-EG-60_11 shows high crystallinity and large particle size compared to Pt-EG-30_11 (4.96 nm compare to 4.23 nm) with the presence of EG or Pt-60_11 (6.58 nm) compare to Pt-30_11 (5.96 nm) without EG. This observation is then confirmed by calculating the average particle size from histogram of particle size distribution (Fig. 4), and the average size of Pt particles was shown in Table 3. The influence of temperature could be explained as follows: at a lower temperature, the formation of crystal nuclei proceeds more rapidly than the growth of it [16]. Therefore smaller Pt particles were obtained at 30 °C compared to this obtained at 60 °C.

Besides, the Pt/C-EG-30_6.5 catalyst has been synthesized in pH = 6.5 solution, compare to Pt/C-EG-30_11 catalyst (the same synthesis conditions, unlike pH), the size of Pt particles in Pt/C-EG-30_6.5 catalyst is larger than the size of Pt particles in Pt/C-EG-30_11 catalyst. Bonnemant et al. reported that Pt nanoparticles are stabilized via electrosteric repulsion between the anionic surface of the Pt nanoparticle and the stabilizer [17]. In the acidic solution, a large number of H⁺ ions interact with negatively charged Pt particles resulting in the destruction of electrosteric repulsion and leading to the growth of Pt nanoparticles. In the basic solution, almost no species would directly interact with negatively charged Pt nanoparticles, which implied that the electrosteric stabilization is unbroken [17, 18]. A similar feature has also been observed in the synthesis of Pt-based metal nanoparticles using EG as a reducing agent [19, 20]. In our case, the size of Pt nanoparticles of Pt/C-EG-30_6.5 sample is about 7.72 nm (Table 2) (estimated from the Scherrer formula at Pt (111) peak) or 6.08 nm (Table 3) (from histogram of particle size distribution (Fig. 4)). The differences in Pt particles between Pt/C-EG-30_6.5 and Pt/C-EG-30_11 can also be explained by the effect of electrosteric repulsion. Under high pH conditions, only minor interaction occurred between H⁺ ions and stabilizer anions, yet the stabilizer strongly interacted with the reduced Pt nanoparticles. Therefore, the growth of Pt particles was significantly restrained, leading to the formation of Pt nanoparticles with smaller size in the Pt/C-EG-30_11 than in the Pt/C-EG-30_6.5 catalyst.

Table 3. The average particle size and surface area were estimated from (***) and (**).

Catalysts	d_{TEM} (nm)	S_{TEM} (m ² /g _{Pt})
Pt/C-30_11	5.96	47
Pt/C-EG-30_11	4.23	66.3
Pt/C-EG-30_6.5	6.08	46
Pt/C-EG-60_11	4.96	56.5
Pt/C-60_11	6.58	42.6

From TEM pictures, estimating the average surface area of Pt nanoparticles on carbon support can also be carried out (Table 3), these result is corresponding to the XRD data that has been shown previously. The distribution and difference in the size of the catalyst particles strongly influenced the activity of the Pt/C catalysts. With the smallest size (4.23 nm), electrochemical active surface area of Pt in the Pt/C-EG-30_11 catalyst sample is largest (66.3 m²/g_{Pt}).

3.3. Cyclic Voltammetry (CV) results

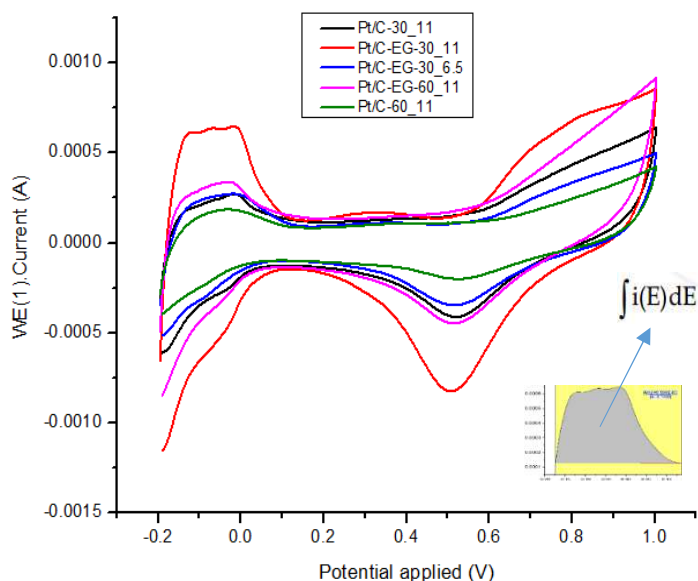


Figure 5. Cyclic voltammograms (CVs) for patterns of 40 wt% Pt/C catalysts were recorded in a N_2 -saturated 0.5 mol/L H_2SO_4 solution (50 mV/s, 25 °C).

The catalyst ink consist of 2.5 mg of Pt/C 40 wt%, 1.0 ml ethanol (C_2H_5OH) and 10 μ l nafion 5 % solution were ultrasonicated in 30 minutes, a homogeneous solution ink was obtained. A small volume (15 μ l/3 pipetting times) of this solution was pipetted onto a 6 mm diameter electrode containing a 3.2 mm diameter glassy carbon (GC) electrode and allowed to dry at room temperature for 30 min (10 min/pipetting once). The platinum loading on GC surface is 0.01 mg (about 0.125 $mg.cm^{-2}$). A three-electrodes cell was used in which the counter electrode was platinum, the reference electrode was Ag/AgCl and working electrode was GC. In the CV measurements, the potential values were converted automatically to normal hydrogen electrode (NHE) [21]. The CV curves were conducted in a N_2 -saturated 0.5 mol/L H_2SO_4 solution, the potential range from -0.2 to 1.0 V with scan rate 50 mV/s at room temperature and measured by the Autolab PGSTAT302N potentiostat/galvanostat, Metrohm Autolab brand.

Figure 5 is CV curves of Pt/C catalysts in H_2SO_4 0.5M solution. From the CV curves, it was easy to calculate the charge of the electrochemical processes which occur on the catalyst particles by integrating. As a result, the electrochemical surface area (ESA) showing the activity of the catalysts was estimated by the following formula [22,23]:

$$S_{ESA-H} = \frac{Q_H}{[Pt] \times Q_{monolayer}} = \frac{\frac{1}{v} \times \int i(E)dE}{[Pt] \times 2.1}$$

where, S_{ESA-H} is electrochemically active surface area (m^2/g_{Pt}), Q_H is the charge for hydrogen desorption (C or A.s), $\int i(E)dE$ is integral of part hydrogen desorption (A.V), 2.1 is $Q_{monolayer}$ ($C.cm^{-2}$) (the charge related to the adsorption or desorption of a hydrogen monolayer on a polycrystalline Pt surface), v is scan rate ($mV.s^{-1}$) and $[Pt]$ represents the platinum loading in the electrode (g). The resultant ESA values are listed in Table 4.

Table 4. The average particle size and surface areas calculated from the Pt crystalline size (S_{XRD}), Pt particles size (S_{TEM}) and electrochemically active surface area (S_{ESA-H}):

Catalysts	S_{ESA-H} (m^2/g_{Pt})
Pt/C-30_11	21.9
Pt/C-EG-30_11	95.2
Pt/C-EG-30_6.5	31.3
Pt/C-EG-60_11	31.4
Pt/C-60_11	15.4

On the CV curves (Fig. 5), there are the electrochemical peaks corresponding to the different electrochemical reactions on the samples' surface. In the potential range about -0.15 – 0.15 V, the peaks express the adsorption/desorption processes of hydrogen on Pt crystal. The mechanism of these processes may take place by two stages. In the forward scan, the potential range from 0.15 to 0.58 V corresponds to the charge of the double layer by the oxygenated groups on the carbon support surface. At the potential 0.65 V, the oxidation process of Pt metal happens to form Pt oxides. Corresponding with this process, there is a reduction peak at 0.51 V of reduction process of Pt–O in the reverse scan [24, 25]. Among the peaks of the catalyst samples, those without EG or pH = 6.5 (acidic solution) are smaller than samples with EG and pH = 11 (basic solution). This means that the activity of these samples is relatively low. The activity of the catalyst synthesized with EG, pH = 11 at the room temperature (Pt/C-EG-30_11) is the highest. The calculated ESA values of the catalyst samples are shown in table 4. The difference in ESA value may be due to the difference in the size of Pt particles. With the biggest size of particles, the ESA value of the Pt/C-60_11 sample is the smallest ($15.4 m^2/g_{Pt}$) corresponding to desorption peak lowest. Possessing the smallest size, the ESA value of the Pt/C-EG-30_11 sample is highest ($95.2 m^2/g_{Pt}$). These results provide an extremely significant information about the relationship between the size and activity of the Pt nanoparticles catalyst on carbon support: The catalysts with smaller particle size will give a higher activity due to larger surface area. This trend also corresponds with the results of TEM and XRD analysis.

4. CONCLUSIONS

Through the influence of the synthesis conditions as temperature, pH and ethylene glycol on size and dispersion of platinum nanoparticles catalyst on carbon support were studied in this work, we found that the electrochemical surface area (ESA) was strongly influenced by the size and the size distribution of the Pt nanoparticles catalyst. As desired, the particle size and the distribution of Pt on carbon support can be controlled through adjusting synthesis conditions such as the temperature, EG enhancer and pH parameter. The results of this study showed the presence of EG with the function as a weak reducing agent and the stabilizer could enhance the distribution and make smaller Pt size compared to the sample without using EG. In addition, the effect of temperature on the Pt/C preparation was studied at room temperature and 60 °C, we also found that when the temperature increases from room temperature to 60 °C, there is a significant difference about the crystallinity and the particles size of Pt on carbon. Finally, the effect of pH parameter on Pt/C electrocatalyst indicated that the basic solution is better than acidic solution for synthesizing this catalyst. The results of this work showed the way to control

size and distribution of Pt catalyst on carbon support that can be used to enhance the activity of Pt/C catalyst with high loading for fuel cell applications.

Acknowledgment. This work was supported by Ho Chi Minh City University of Technology, University Of Science Ho Chi Minh City, Ho Chi Minh City University of Natural Resources and Environment.

REFERENCES

1. Hamnett A. - Mechanism and electrocatalysis in the directmethanol fuel cell, *Catalysis Today* **38** (1997) 445–457.
2. Markovic N. M., Ross Jr. P. N. - Surface science studies of model fuel cell electrocatalysts, *Surface Science Reports* **45** (2002) 117–229.
3. Armadi I. S., Wang Z. L., Green T. C., Henglein A., El-Sayed M. A. - Shape-Controlled Synthesis of Colloidal Platinum Nanoparticles, *Science* **272** (1996) 1924–1926.
4. Singh R. N., Awasthi R. and Sharma C. S. - Review: An Overview of Recent Development of Platinum Based Cathode Materials for Direct Methanol Fuel Cells, *Int. J. Electrochem. Sci.* **9** (2014) 5607–5639.
5. Liu Z. L., Lee J. Y., Han M., Chen W. X. and Gan L. M. - Synthesis and characterization of PtRu/C catalysts from microemulsions and emulsions, *J. Mater. Chem.* **12** (2002) 2453–2458.
6. Okitsu K., Yue A., Tanabe S., Matsumoto H. - Sonochemical preparation and catalytic behavior of highly dispersed palladium nanoparticles on alumina, *Chem. Mater.* **12** (2000) 3006–3011.
7. Tu W. and Liu H. - Rapid synthesis of nanoscale colloidal metal clusters by microwave irradiation, *J. Mater. Chem.* **10** (2000) 2207–2211.
8. Komarneni S., Li D., Newalkar B., Katsuki H., Bhalla A. S. - Microwave-polyol process for Pt and Ag nanoparticles, *Langmuir* **18** (2002) 5959–5962.
9. Coutanceau C., Baranton S. and Napporn T.W.. Platinum Fuel Cell Nanoparticle Syntheses: - Effect on Morphology, Structure and Electrocatalytic Behavior, *The Delivery of Nanoparticles*, Dr. Abbass A. Hashim (Ed.), InTech, Chapter **19** (2012) 403–426.
10. Senthil Kumar S. M., Hidyatai N., Herrero J. S., Irusta S., Scott K. - Efficient Tuning of the Pt Nano-Particle Mono Dispersion on Vulcan XC-72R by Selective Pre - Treatment and Electrochemical Evaluation of Hydrogen Oxidation and Oxygen Reduction Reactions, *International journal of hydrogen energy* **36** (2011) 5453–5465.
11. Lazaro M. J., Celorrio V., Calvillo L., Pastor E. and Moliner R. - Influence of the synthesis method on the properties of Pt catalysts supported on carbon nanocoils for ethanol oxidation, *Journal of Power Sources* **196** (2011) 4236–4241.
12. Shah M. A. - Growth of uniform nanoparticles of platinum by an economical approach at relatively low temperature, *Scientia Iranica F* **19** (2012) 964–966.
13. Zhou W. J., Li W. Z., Song S. Q., Zhou Z. H., Jiang L. H., Sun G. Q., Xin Q., Poulianitis K., Kontou S., Tsiakaras P. - Bi- and tri-metallic Pt-based anode catalysts for direct ethanol fuel cells, *Journal of Power Sources* **131** (2004) 217–223.
14. Joo J. B., Kim P., Kim W., Kim Y., Yi J. - Effect of the preparation conditions of carbon-supported Pt catalyst on PEMFC performance, *J. Appl. Electrochem.* **39** (2009) 135–140.

15. Kim P., Joo J. B., Kim W., Kim J., Song I. K., Yi J. - NaBH₄-assisted ethylene glycol reduction for preparation of carbon-supported Pt catalyst for methanol electrooxidation, *Journal of Power Sources* **160** (2006) 987–990.
16. Tian J. H., Wang F. B., Shan ZH. Q., Wang R. J. and Zhang J. Y. - Effect of preparation conditions of Pt/C catalysts on oxygen electrode performance in proton exchange membrane fuel cells, *Journal of Applied Electrochemistry* **34** (2004) 461–467.
17. Bonnemann H., Braun G., Brijoux W., Brinkmann R., Schulze Tilling A., Seevogel K., Siepen K. - Nanoscale colloidal metals and alloys stabilized by solvents and surfactants - Preparation and use as catalyst precursors, *Journal of Organometallic Chemistry* **520** (1996) 143–162.
18. Oh H. -S., Oh J. -G., Hong Y. -G., Kim H. - Investigation of carbon-supported Pt nanocatalyst preparation by the polyol process for fuel cell applications, *Electrochimica Acta* **52** (2007) 7278–7285.
19. Zhou Z., Zhou W., Wang S., Wang G., Jiang L., Li H., Sun G., Xin Q. - Preparation of highly active 40 wt.% Pt/C cathode electrocatalysts for DMFC via different routes, *Catalysis Today* 93–95 (2004) 523–528.
20. Bock C., Paquet C., Couillard M., Botton G. A., MacDougall B. R. - Size-Selected Synthesis of PtRu Nano-Catalysts: Reaction and Size Control Mechanism, *Journal of the American Chemical Society* **126** (2004) 8028–8037.
21. Khan A., Nath B. K., and Chutia J. - Nanopillar structured Platinum with enhanced catalytic utilization for electrochemical reactions in PEMFC, *Electrochimica Acta* **146** (2014) 171–177.
22. Pozio A., De Francesco M., Cemmi A., Cardellini F., Giorgi L. - Comparison of high surface Pt/C catalysts by cyclic voltammetry, *Journal of Power Sources* **105** (2002) 13–19.
23. Perez J., Gonzalez E. R., Ticianelli E.A. - Oxygen electrocatalysis on thin porous coating rotating platinum electrodes, *ElectrochimicaActa* **44** (1998) 1329–1339.
24. Takahashi I. and Kocha S. S. - Examination of the activity and durability of PEMFC catalysts in liquid electrolytes, *Journal of Power Sources* **195** (2010) 6312–6322.
25. Chaparro A. M., Martin A. J., Folgado M. A., Gallardo B. and Daza L. - Comparative analysis of the electroactive area of Pt/C PEMFC electrodes in liquid and solid polymer contact by underpotential hydrogen adsorption/desorption, *International Journal of Hydrogen Energy* **34** (2009) 4838–4846.